

Honeycomb Pattern Formation by Laser-Beam Filamentation in Atomic Sodium Vapor

Ryan S. Bennink, Vincent Wong, Alberto M. Marino, David L. Aronstein, Robert W. Boyd,
C. R. Stroud, Jr., and Svetlana Lukishova

The Institute of Optics, University of Rochester, Rochester, New York 14627

Daniel J. Gauthier

Department of Physics, Duke University, Durham, North Carolina 27708

(Received 26 July 2001; revised manuscript received 16 November 2001; published 27 February 2002)

We have observed transverse pattern formation leading to highly regular structures in both the near and far fields when a near-resonant laser beam propagates without feedback through an atomic sodium vapor. One example is a regular far-field honeycomb pattern, which results from the transformation of the laser beam within the vapor into a stable three-lobed structure with a uniform phase distribution and highly correlated power fluctuations. The predictions of a theoretical model of the filamentation process are in good agreement with these observations.

DOI: 10.1103/PhysRevLett.88.113901

PACS numbers: 42.65.Sf, 42.50.-p, 45.70.Qj, 89.75.Kd

In this Letter we describe our observation of a striking form of optical pattern formation in which a single laser beam breaks up into a stable, regularly structured beam in passing without feedback through a sodium vapor cell. Pattern formation [1] in optical systems [2] is an area of widespread interest, both from the conceptual point of view of understanding how regular patterns can emerge from uniform or randomly structured input fields and from the practical point of view of utilizing such patterns in image formation and manipulation. Applications include the use of imaging techniques that exploit the quantum nature of the light field to increase the sensitivity or resolution of optical systems [3,4], the construction of optical neural networks and associative memories [5], and the use of fractal and wavelet algorithms for image compression [6].

In our experiment (Fig. 1), the laser beam undergoes filamentation [7] and breaks up into three nearly equally spaced components of comparable intensity in passing through the sodium interaction region. The far-field pattern consists of the coherent superposition of the diffraction pattern from each of the three beams and thus has the form of the honeycomb pattern (the Fourier transform of the near-field pattern) which is also shown in the figure. Note that the k -space distribution of the optical field within the interaction region possesses this same honeycomb structure; our procedure of observing the pattern in the far field is simply a convenient way of monitoring the k -space distribution of the field within the interaction region. In the particular example of Fig. 1, the pattern was produced by a cw dye laser beam containing 150 mW of power detuned 2 GHz to the high-frequency side of the sodium D2 resonance line. This beam was focused to a beam waist near the sapphire entrance window of a 7-cm-long vapor cell. The cell contained no buffer gas and was operated at a temperature of 220 °C and thus contained 8×10^{12} atoms per cm^3 . As described in detail below, the various regions of the near-field pattern exhibit strong phase and power correlations, which show that the nonlinear interaction leading

to this form of pattern formation fully maintains the coherence of the optical field.

Pattern formation has been observed in a wide variety of material systems, including atomic vapors, liquid crystals, $\chi^{(2)}$ crystals, photorefractive materials, organic liquids, glasses, semiconductors, and biological materials, as reviewed in the literature [2]. Our particular concern is pattern formation in atomic vapors [8]. Observations of these patterns have often involved systems possessing some sort of optical feedback such as a single feedback mirror [9], resonators [10], or wave mixing of counter-propagating beams [11]. The patterns we observe, however, occur in a homogeneous medium without feedback. In all of our experiments, the laser beam was made to enter the cell at slightly oblique incidence to avoid feedback

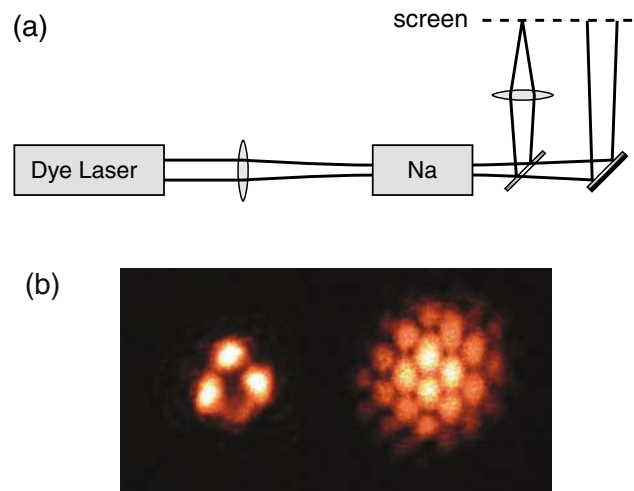


FIG. 1 (color). (a) Experimental setup used to study optical pattern formation; patterns were recorded both in the near and far fields. Typical conditions were input power, 150 mW; input beam diameter, 160 μm ; laser frequency, 2 GHz blue-detuned from the sodium D2 line; cell length, 7 cm; and number density, $8 \times 10^{12} \text{ cm}^{-3}$. (b) Example of pattern formation as observed in the near field (left) and far field (right).

due to reflections from the cell windows, and we verified that the patterns did not vary with the incidence angle. Moreover, most previously reported patterns exhibiting a hexagonal tile structure occurred at the exit face of the nonlinear medium [12], whereas the honeycomb pattern reported here occurs in the far zone of the transmitted field [13]. We note that Vaupel *et al.* [14] observed patterns in the far zone of the field generated by an optical parametric oscillator (that is, in the presence of feedback), and that several researchers [15] observed spatial instabilities of a single laser beam passing through an atomic vapor but did not report observation of hexagon formation in the far field. In summary, we are unaware of previous observations of honeycomb (hexagonal) pattern formation in the far field from a single beam passing through an atomic medium without feedback.

In addition to the honeycomb pattern illustrated in Fig. 1(b), we have observed a wide variety of other patterns in our experiment. Some of these patterns are shown in Fig. 2. Figure 2(a) shows how the near-field and k -space patterns evolve as the incident laser power is increased at a fixed number density of $3 \times 10^{12} \text{ cm}^{-3}$, a blue detuning of 2 GHz, and an input Gaussian-beam spot size of $2w_0 = 180 \text{ mm}$. The beam exiting the cell is unstructured at low powers, shrinks in size as the power is increased, and at an input power of approximately 80 mW begins to form three distinct spots, leading to hexagonal cells in the far field. As the power is increased further, the near-field spots move farther apart, and thus the size of the cells of the honeycomb pattern decreases. Above approximately 150 mW, the beam contains enough power to generate additional filaments, leading to a far-field

distribution that is highly structured but contains no apparent regular order. At our highest accessible input power of 400 mW, as many as eleven near-field spots were observed. Figure 2(b) shows how the pattern evolves as we change the laser frequency at a fixed incident power of 100 mW, again for a number density of $3 \times 10^{12} \text{ cm}^{-3}$ and an input spot size of 180 mm. We see that the beam exiting the cell retains its near-Gaussian transverse structure when the laser frequency is far from resonance, and that the beam first develops a small “hot” center as resonance is approached. With decreasing detuning (and hence increasing nonlinearity), the beam develops rings in both the near and far fields and eventually breaks up into a pattern with threefold symmetry. Figure 2(c) shows the laser-frequency dependence of the pattern formation under slightly different conditions, with a number density of $8 \times 10^{12} \text{ cm}^{-3}$ and a power of 47 mW. In this case the beam preferentially develops a two-lobed rather than a three-lobed structure, with corresponding stripes in the far field. The results shown in Fig. 2 indicate that honeycomb pattern formation occurs only under fairly restricted experimental conditions. We speculate that it is for this reason that this effect has not previously been reported in the literature.

The patterns we have observed, and in particular those shown in Fig. 1(b), are remarkably stable and show no variation in structure over time scales of tens of minutes. This observation suggests that these patterns may constitute “quantum images” (that is, field distributions containing strong spatial quantum correlations) as described by Lugiato and coworkers [4]. In fact, theoretical arguments [16] show that strong quantum correlations are expected to be produced by those interactions that lead to patterns with hexagonal symmetry. We have studied further the stability of these patterns by examining the coherence properties of the transmitted light field. Figure 3 shows an interferogram of the near-field light distribution, superimposed with a contour map of the near-field intensity distribution, taken under conditions similar to those of Fig. 1(b). This pattern was formed by interfering the field leaving the cell with a (nearly planar) reference wave front inclined at a slight angle to produce (slightly curved) tilt fringes. The brightest portions of the interferogram were allowed to saturate the CCD camera so that we could follow the fringes far into the wings of the light distribution associated with each filament. The existence of stationary, high-contrast fringes indicates that the transmitted light is predominantly at the same frequency as the input light. In addition, the even spacing of the fringes indicates that the transmitted light field has an essentially uniform phase across its entire transverse profile. Normally one would expect the phase of a light field transmitted through a strongly nonlinear medium to be highly nonuniform as a consequence of transverse intensity variations. The uniformity of the phase in the present case is reminiscent of similar behavior that occurs in the formation of optical solitons, although we stress that we have no

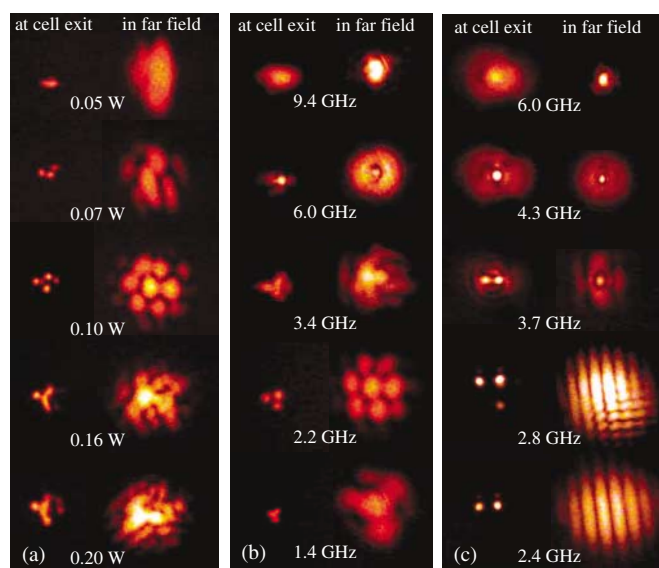


FIG. 2 (color). Near- and far-field intensity distributions of the light leaving the sodium cell as functions of (a) laser power and (b),(c) laser frequency. (a) $N = 3 \times 10^{12} \text{ cm}^{-3}$, $\Delta/2\pi = 2 \text{ GHz}$. (b) $N = 3 \times 10^{12} \text{ cm}^{-3}$, $P = 0.11 \text{ W}$. (c) $N = 8 \times 10^{12} \text{ cm}^{-3}$, $P = 0.05 \text{ W}$. In all cases the input beam diameter was $2w = 0.18 \text{ mm}$ and the propagation length was 7 cm.

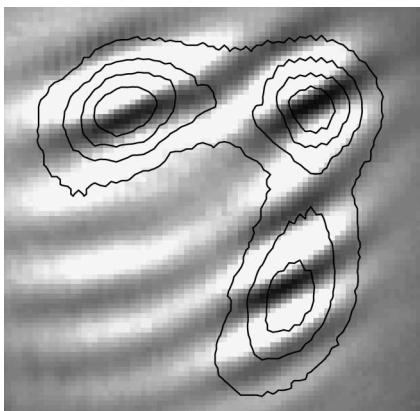


FIG. 3. Interferogram of the near-field light distribution for a case in which three filaments are formed, superimposed with a contour map of the filament intensity. Note that the light leaving the interaction region has a nearly uniform phase distribution.

direct evidence that soliton formation is occurring in our experiment.

We have also found that the light leaving the sodium interaction region possesses strong spatial correlations. In performing this measurement we adjusted the input conditions [see Fig. 2(c)] so that in the near field the output consists of two spots carrying nearly equal power. We find that the noise in the difference of the two output intensities is smaller than the noise in the sum of the two output intensities, showing that the two components of the output are correlated in their fluctuations. Efforts to lower the noise floor of our detection apparatus and test the degree of correlation at the level of the standard quantum limit are in progress.

Our experimental observations are in good agreement with the predictions of standard models of nonlinear optical self-action effects. A key parameter that determines the properties of self-action effects is the critical power for self-focusing, which is given by $P_{cr} = \lambda^2/8n_2$, where n_2 is the coefficient of the intensity dependent refractive index. It is well known that self-focusing can occur only if the laser power exceeds P_{cr} , and that (to first approximation) the process of filamentation leads to the creation of multiple components, each containing power P_{cr} . Under our typical experimental conditions of a number density of $N = 8 \times 10^{12}$ and a detuning of $\Delta/2\pi = 2$ GHz, the optical constants of sodium vapor have the values [17] $\chi^{(1)} = 1.6 \times 10^{-5}$ esu, $\chi^{(3)} = 2.5 \times 10^{-6}$ esu, $n_2 = 9 \times 10^{-8}$ cm² W⁻¹, and $I_{sat} = 1.6$ kW cm⁻². The critical power under these conditions is thus given by $P_{cr} = 5.0$ mW, in good qualitative agreement with the measured power of 2.0 mW of each spot in Fig. 3. The intensity of the light within each spot in Fig. 3 (of diameter 30 μ m at the exit window) is 0.7 kW cm⁻². This value is less than but of the order of the calculated value of the saturation intensity quoted above and supports the view that incipient saturation of the nonlinear optical response has limited the further collapse of the optical filaments under our experimental conditions.

To establish more explicitly the origin of pattern formation in our experiment, we have performed numerical modeling of pattern formation in the propagation of a laser field through a saturable [18] nonlinear optical medium. We begin with the scalar wave equation in the form

$$\left(2ik \frac{\partial}{\partial z} + \nabla_T^2\right)E = -4\pi k^2 \frac{\chi^{(1)}}{1 + |E/E_{sat}|^2} E, \quad (1)$$

where $E = E(x, y, z)$ is the electric field envelope function and E_{sat} is the saturation field amplitude. We solve this equation numerically on a 96×96 transverse grid under conditions similar to those of our experiment. The input field was seeded with 3%, spatially δ -correlated amplitude noise. A typical outcome of the calculation is shown in Fig. 4. The beam initially undergoes strong self-focusing, followed by oscillations and the development of rings. After ejecting some filaments that disperse in the transverse dimensions, the beam breaks up into three peaks that maintain their size and shape as they slowly drift apart. This behavior is similar to that described earlier by Firth and Skryabin [19]. We find that different realizations of the input noise lead to filaments with varying sizes and relative positions, but that the final number of filaments is nearly always 3 for the specified input conditions. Furthermore, it is found that this three-way filamentation occurs only for input Gaussian beams whose radius and peak intensity are nearly equal to those given above. For slightly weaker input beams we find that the filamentation process favors the development of two spots, whereas for stronger input

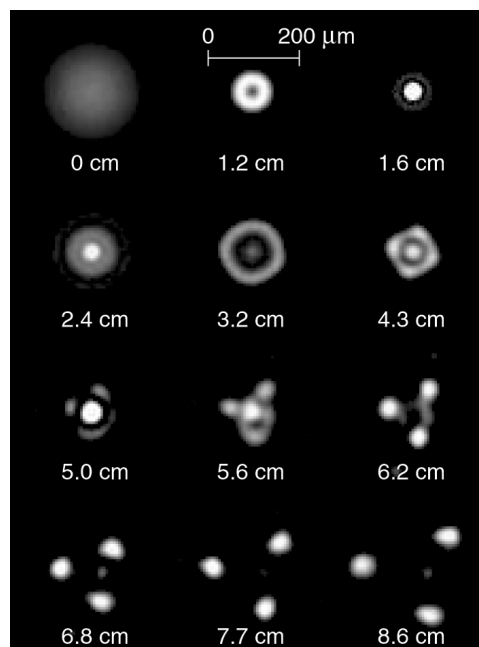


FIG. 4. Numerical calculation of the propagation of a near-Gaussian laser beam through a medium with a saturable nonlinear response. The beam is seen to break up into three filaments, in agreement with the experimental observations presented in Fig. 1. The input conditions are those of the experiment, namely the peak input intensity is 4 times the saturation intensity and the beam diameter is 0.13 mm.

beams more than three spots are created. In performing the calculation shown in Fig. 4, we took the input beam to have a peak intensity of 4 times the saturation intensity and took the input (Gaussian) beam diameter to be $130 \mu\text{m}$, where the measured value is $180 \mu\text{m}$. This agreement is quite reasonable in light of the fact that our theoretical model does not treat the multilevel structure of the sodium atom.

In summary, we have observed a dramatic example of optical pattern formation in which a single laser beam propagating through atomic sodium vapor without feedback develops a stable, regular transverse structure. In particular, a three-filament near-field pattern leading to a honeycomb far-field pattern occurs at intensities near the saturation intensity and at powers larger than (but of the order of magnitude of) the critical power for self-focusing. The three-filament pattern has a uniform phase profile and strongly correlated power fluctuations, which suggest that it is perhaps a quantum image. These observations are also in good agreement with numerical simulations of filamentation in a two-level medium.

This work was supported by ONR Grant No. N00014-99-1-0539. D.J.G. gratefully acknowledges the support of NSF Grant No. PHY-9876988. The authors gratefully acknowledge fruitful discussions on the contents of this paper with W.J. Firth, H.M. Gibbs, G. Khitrova, F.A. Narducci, K.J. Parker, and A.M. Tekalp.

-
- [1] M. Cross and P. Hohenberg, *Rev. Mod. Phys.* **65**, 851 (1993).
- [2] See, for instance, the special issues of *J. Opt. Soc. Am. B* [7, Nos. 6 and 7 (1990)] dealing with transverse effects in nonlinear optical systems and, especially, the overview article by N. B. Abraham and W. J. Firth, *J. Opt. Soc. Am. B* **7**, 951 (1990). See also *Self-Organization in Optical Systems and Applications in Information Technology*, edited by M. A. Vorontsov and W. B. Miller (Springer, Berlin, 1995).
- [3] V. L. Koval'chuk *et al.*, *Sov. J. Quantum Electron.* **7**, 495 (1977); L. A. Lugiato *et al.*, *Philos. Trans. R. Soc. London A* **354**, 767 (1996); S. K. Choi, M. Vasilyev, and P. Kumar, *Phys. Rev. Lett.* **83**, 1938 (1999); M. I. Kolobov and C. Fabre, *Phys. Rev. Lett.* **85**, 3789 (2000); A. N. Boto *et al.*, *Phys. Rev. Lett.* **85**, 2733 (2000); G. S. Agarwal *et al.*, *Phys. Rev. Lett.* **86**, 1389 (2001).
- [4] A. Gatti and L. Lugiato, *Phys. Rev. A* **52**, 1675 (1995); I. Marzoli, A. Gatti, and L. A. Lugiato, *Phys. Rev. Lett.* **78**, 2092 (1997).
- [5] J. J. Hopfield, *Proc. Natl. Acad. Sci. U.S.A.* **79**, 2554 (1982); J. H. Hong and D. Psaltis, in *Contemporary Nonlinear Optics*, edited by G. P. Agrawal and R. W. Boyd (Academic Press, San Diego, 1992).
- [6] M. F. Barnsley, *Fractals Everywhere* (Academic Press, Boston, 1988); M. Vetterli and J. Kovacevic, *Wavelets and Subband Coding* (Prentice Hall, Englewood Cliffs, NJ, 1995).
- [7] Throughout this Letter we use the term filamentation to mean simply the breakup of a laser beam into multiple transverse components by means of nonlinear optical self-action effects. This is the sense used recently, for instance, by S. Tzortzakis *et al.*, *Phys. Rev. Lett.* **86**, 5470 (2001). It should be noted that some workers use the word filamentation in a different, more restricted sense to mean the breakup of a beam into one or more components which subsequently propagate stably through the material system as spatial solitons.
- [8] J. E. Bjorkholm and A. Ashkin, *Phys. Rev. Lett.* **32**, 129 (1974); D. J. Harter, P. Narum, M. G. Raymer, and R. W. Boyd, *Phys. Rev. Lett.* **46**, 1192 (1981); D. J. Gauthier, M. S. Malcuit, A. L. Gaeta, and R. W. Boyd, *Phys. Rev. Lett.* **64**, 1721 (1990); J. Pender and L. Hesselink, *J. Opt. Soc. Am. B* **7**, 1361 (1990); M. Kauranen *et al.*, *Opt. Lett.* **16**, 943 (1991); A. Petrossian *et al.*, *Europhys. Lett.* **18**, 689 (1992); B. Rhrich, T. Ackerman, and W. Lange, *Appl. Phys. B* **72**, 21 (2001).
- [9] G. Grynberg, A. Maître, and A. Petrossian, *Phys. Rev. Lett.* **72**, 2379 (1994); G. D'Alessandro and W. J. Firth, *Phys. Rev. Lett.* **66**, 2597 (1991); B. Schapers *et al.*, *Phys. Rev. Lett.* **85**, 748 (2000).
- [10] K. Staliunas and V. J. Sánchez-Morcillo, *Opt. Commun.* **177**, 389 (2000).
- [11] D. J. Gauthier *et al.*, *Phys. Rev. Lett.* **61**, 1827 (1988); G. Grynberg *et al.*, *Opt. Commun.* **67**, 363 (1988); M. Le Berre *et al.*, *Phys. Rev. A* **43**, 6345 (1991); A. L. Gaeta *et al.*, *J. Opt. Soc. Am. B* **6**, 1709 (1989).
- [12] F. Papoff *et al.*, *Phys. Rev. A* **48**, 634 (1993); R. MacDonald and H. Danilewski, *Mol. Cryst. Liq. Cryst.* **251**, 145 (1994); R. Herrero *et al.*, *Phys. Rev. Lett.* **82**, 4627 (1999).
- [13] Far-field hexagonal pattern formation was observed previously in photorefractive crystals, where the nature of the nonlinear coupling is quite different from that of our experiment. See, for instance, P. M. Lushnikov and A. V. Mamaev, *Opt. Lett.* **24**, 1511 (1999); A. V. Mamaev and M. Saffman, *Opt. Lett.* **22**, 283 (1997); S. G. Odulov, M. Yu. Goulikov, and O. A. Shinkarenko, *Phys. Rev. Lett.* **83**, 3637 (1999).
- [14] M. Vaupel, A. Maître, and C. Fabre, *Phys. Rev. Lett.* **83**, 5278 (1999).
- [15] D. Grischkowsky, *Phys. Rev. Lett.* **24**, 866 (1970); J. W. Grantham, H. M. Gibbs, G. Khitrova, J. F. Valley, and Xu Jiajin, *Phys. Rev. Lett.* **66**, 1422 (1991); B. D. Paul, M. L. Dowell, A. Gallagher, and J. Cooper, *Phys. Rev. A* **59**, 4784 (1999).
- [16] G. Grynberg and L. A. Lugiato, *Opt. Commun.* **101**, 69 (1993); A. Gatti and S. Mancini, *Phys. Rev. A* **65**, 013816 (2002).
- [17] R. W. Boyd, *Nonlinear Optics* (Academic Press, Boston, 1992). See, for instance the numerical example presented at the end of Section 5.3.
- [18] J. M. Soto-Crespo, E. M. Wright, and N. N. Akhmediev, *Phys. Rev. A* **45**, 3168 (1992).
- [19] W. J. Firth and D. V. Skryabin, *Phys. Rev. Lett.* **79**, 2450 (1997).